Predictions

The model proposed here predicts that each T cell carries three receptor molecules. Two of these are non-antibody receptors, at least one of which is specific for a self-MHC molecule (either K, D or I in the mouse). Detection and characterisation of R anti-H molecules would provide evidence for the model. A small fraction of T-cell clones responding to a foreign antigen recognised together with a self-H antigen will also be able to recognise the antigen presented with an allo-H antigen due to the postulated third receptor (R anti-allo-H). Evidence for the latter subset of T-cell clones has been published[31].

Receptors specific for self-MHC are postulated to be the products of a multigene family encoding receptors for many allo-MHC products. The extent of that gene family will be revealed by further tests of the ability of pre-T cells to be selected in the thymus for recognition of a range of MHC types as self. Because expression of receptors for self-MHC molecules is postulated to be selected by the MHC antigens of the thymus the MHC appears to code for the T-cell receptor. An involvement of anti-self-MHC receptors in I-region linked non-responsiveness is postulated.

While recognising that I have invoked a new gene family that may or may not exist, I trust that the concept has some merit in ordering existing data and that it may influence future experimental design.

I thank Andrew McMichael, Dale Kipp and John Shire for stimulating and helpful discussion.

1. Zinkernagel, R. M. & Doherty, P. C. *Nature* **251,** 547–548 (1974).
2. Shearer, G. M., Rhem, T. G. & Garbarino, C. A. *J. exp. Med.* **141,** 1348–1364 (1975).
3. Bevan, M. J. *J. exp. Med.*, **142,** 1349–1364 (1975).
4. Shevach, E. M. & Rosenthal, A. S. *J. exp. Med.* **138,** 1213–1227 (1973).
5. Katz., D. H. & Benacerraf, B. *Transplantn Rev.* **22,** 175–195 (1975).
6. Bechtol, K. B., Freed, J. H., Herzenberg, L. A. & McDevitt, H. O. *J. exp. Med.* **140,** 1660–1675 (1974).
7. von Boehmer, H., Hudson, L. & Sprent, J. *J. exp. Med.* **142,** 989–997 (1975).
8. Katz, D. H. *Cold Spring Harb. Symp. quant. Biol.* **41,** 611–624 (1976).
9. Doherty, P. C. *Immunogenetics* **3,** 517–524 (1976).
10. Bevan, M. J. *Cold Spring Harb. Symp. quant. Biol.* **41,** 519–527 (1976).
11. von Boehmer, H., Haas, W. & Jerne, N. K. *Proc. natn. Acad. Sci. U.S.A.* **75,** 2439–2442 (1978).
12. Bevan, M. J. *Nature* **269,** 417–419 (1977).
13. Zinkernagel, R. M., Callahan, G. N., Klein, J. & Dennert, G. *Nature* **271,** 251–253 (1978).
14. Zinkernagel, R. M. *et al. J. exp. Med.* **147,** 882–896 (1978).
15. Jerne, N. K. *Eur. J. Immun.* **1,** 1–9 (1971).
16. Bodmer, W. F. *Nature* **237,** 139–145 (1972).
17. Sprent, J. *J. exp. Med.* **147,** 1159–1174 (1978).
18. Cohn, M. & Epstein, R. *Cell. Immun.* **39,** 125–153 (1978).
19. Janeway, C. A., Jr, Binz, H. & Wigzell, H. *Scand. J. Immun.* **5,** 993–1001 (1976).
20. Rabbits, T. M. & Forster, A. *Cell* **13,** 319–327 (1978).
21. Lenhart-Schuller, R., Hohn, B., Brack, C., Hirama, M. & Tonegawa, S. *Proc. natn. Acad. Sci. U.S.A.* **74,** 4709–4713 (1978).
22. Seidman, J. & Leder, P. *Nature* **276,** 790–795 (1978).
23. Deiner, E. & Water, C. A. in *T and B Lymphocytes: Recognition and Function* (eds Bonavida, B., Vitetta, E. & Bach, F. (Academic, New York, in the press).
24. Matzinger, P. & Mirkwood, G. *J. exp. Med.* **148,** 84–92 (1978).
25. Blanden, R. V. & Kees, U. *J. exp. Med.* **147,** 1661–1670 (1978).
26. Cantor, H. & Boyse, E. A. *J. exp. Med.* **141,** 1376–1389 (1975).
27. Cantor, H. & Boyse, E. A. *J. exp. Med.* **141,** 1390–1399 (1975).
28. Zinkernagel, R. M. & Doherty, P. C. *J. exp. Med.* **141,** 1427–1436 (1975).
29. Blank, K. & Lilley, F. *Nature* **269,** 808–809 (1977).
30. Hurme, M., Hetherington, C. M., Chandler, P. R., Gordon, R. D. & Simpson, E. *Immunogenetics* **5,** 453–459 (1977).
31. Ching, L-M. & Marbrook J. *Eur. J. Immun,* **9,** 22–27 (1979).
32. Simonsen, M. *Cold Spring Harb. Symp. quant. Biol.* **32,** 517–523 (1968).
33. Wilson, D. B., Blyth, J. & Nowell, P. C. *J. exp. Med.* **128,** 1157–1181 (1968).
34. Bach, F. M., Bock, H., Graupner, K., Day, E. & Klostermann, H. *Proc. natn. Acad. Sci. U.S.A.* **62,** 377–384 (1969).
35. Skinner, M. A. & Marbrook J. *J. exp. Med.* **143,** 1562–1567 (1976).
36. Bevan, M. J., Langman, R. & Cohn, M. *Eur. J. Immun.* **6,** 150–156 (1976).
37. Lindahl, K. F. & Wilson, D. B. *J. exp. Med.* **145,** 508–522 (1977).
38. Teh, H-S., Harley, E., Phillips, R. A. & Miller, R. G. *J. Immun.* **118,** 1049–1056 (1977).
39. Brondz, B. D. *Transplantn Rev.* **10,** 112–151 (1972).
40. Ford, W. L. & Atkins, R. C. *Nature new Biol.* **234,** 178–180 (1972).
41. Lefkovits, I. *Curr. Topics Microbiol. Immun.* **65,** 21–58 (1974).
42. Wilson, D. B. in *Progress in Immunology II,* **2** (eds Brent, L. & Holbrow, J.) 145 (1974).
43. Binz, H. & Wigzell, H. *Cold Spring Harb. Symp. quant. Biol.* **41,** 275–284 (1976).
44. Krawinkel, U. *et al. Cold Spring Harb. Symp. quant. Biol.* **41,** 285–294 (1976).
45. Jerne, N. K. *Annals Immun., Paris* **125C,** 373–389 (1974).
46. Sege, K. & Paterson, P. A. *Nature* **271,** 167–168 (1978).
47. Binz, H. & Wigzell, H. *J. exp. Med.* **142,** 1218–1230 (1975).
48. Eichmann, K. *Adv. Immun.* **26,** 195–254 (1978).
49. Langman, R. E. *Rev. Physiol. Biochem. Pharmac.* **81,** 1–37 (1978).
50. Kees, U., Müllbacher, A. & Blanden, R. V. *J. exp. Med.* **148,** 1711–1715 (1978).
51. Meo, T., Vives, J., Miggiano, B. & Shreffler, D. *Transplantn Proc.* **5,** 377–381 (1973).
52. Festenstein, H. *Transplantn* Rev. **15,** 62–88 (1973).
53. Forman, J. & Klein, J. *Immunogenetics* **1,** 469–481 (1975).
54. Benacerraf, B. & McDevitt, H. O. *Science* **175,** 273–279 (1972).
55. Hammerling, G. J. & McDevitt, H. O., *J. Immun.* **112,** 1726–1733 (1974).
56. Ebringer, A., Deacon, N. L. & Young, C. R. *J. Immunogenetics* **3,** 401–409 (1976).
57. Kappler, J. W. & Marrack, P. *J. exp. Med.* **148,** 1510–1522 (1978).

ARTICLES

Observations of flexure and the geological evolution of the Pacific Ocean basin

A. B. Watts & J. H. Bodine

Lamont-Doherty Geological Observatory, and Department of Geological Sciences, Columbia University, Palisades, New York 10964

N. M. Ribe

Department of Geophysical Sciences, University of Chicago, Chicago, Illinois 60637

The response of the Pacific plate to oceanic island and seamount loads has been used to estimate the distribution of ridge crest and off-ridge volcanism on the plate since the late Jurassic. The most extensive event, forming the Hess rise, Line Islands ridge, Necker ridge, and Robbie ridge, occurred on the Pacific/Farallon and Pacific/Phoenix ridge crests during the interval 90–120 Myr BP (Barremian to Turonian). This event, which extended over a much larger area than comparable volcanism on the continents, is one of the largest to be documented in the geological record.

THE Pacific Ocean floor is characterised by numerous oceanic islands and seamounts of mainly volcanic origin[1–4]. Although the age of the oceanic crust of the Pacific basin is now reasonably well known from marine magnetic lineations and Deep Sea Drilling Project (DSDP) sites, the origin and age of these volcanic features are largely unknown. These oceanic islands and seamounts are of geological interest as they are located within the interior of the Pacific plate and may therefore provide information on intra-plate volcanism. This article presents a method, based on oceanic plate flexure, for determining the origin and age of some of these volcanic features in the Pacific Ocean basin.

Lithospheric flexure

The concept of plate tectonics is based on a strong rigid lithosphere which overlies a weaker asthenosphere. The principal evidence for a strong lithosphere on long time scales ($>10^6$ yr) has come from studies of its response to surface loads[5–15]. These studies have shown that in several cases, geological and geo-

0028–0836/80/060532—06$01.00

physical data in the region of surface loads can be explained by a simple model in which the lithosphere responds to long-term loads in a manner similar to that of a thin elastic plate overlying a weak fluid.

The results of recent studies of oceanic plate flexure are summarised in Fig. 1 in which the elastic thickness of the oceanic lithosphere T_e is plotted as a function of the age of the lithosphere at the time of loading. Different types of geological features have been plotted in Fig. 1. The age of the lithosphere at the time of loading was estimated at each feature by subtracting the age of the load from the age of the underlying sea floor. The studies by Watts[9] and McNutt and Menard[10] are shown as dashed lines because a single estimate of T_e was obtained for a wide range of age at the time of loading (>60 Myr). Also shown as a dashed line is the study by Caldwell[14] at the Aleutian trench as it is difficult to separate the Aleutian outer rise from a broad regional rise in bathymetry which occurs seawards of the trench[16]. Figure 1 summarises all recent estimates of T_e, except those from the Philippine and Tonga–Kermadec trenches[14] where the age of the subducting oceanic crust is too poorly known.

The main results shown in Fig. 1 are that surface loads formed on young lithosphere, such as the topography of oceanic Layer 2, are associated with relatively small values of T_e while loads formed on old lithosphere, such as the Hawaiian–Emperor seamount chain, are associated with relatively high values. The simplest interpretation of these results is that as the oceanic lithosphere increases in age it cools, thickens, and becomes more rigid in its response to surface loads. Figure 1 shows that there is good general agreement between T_e and the 300 to 600 °C oceanic isotherms, based on a cooling plate model[17].

As the age of the surface loads plotted in Fig. 1 are in the range of a few Myr to several tens of Myr, Fig. 1 suggests T_e is acquired at the time of loading and does not change appreciably with time. This result is consistent with thermal models which predict that the thickness of the lithosphere increases with age[9] and with inferences of the rheology of the oceanic lithosphere based on extrapolations of data from experimental rock mechanics[18,19].

The results in Fig. 1 have important implications for studies of the geological evolution of the ocean basins. For example, Fig. 1 suggests that an oceanic island or seamount formed on young sea floor would be associated with a relatively small T_e, while an oceanic island or seamount formed on old sea floor would be associated with a relatively large T_e. Thus by determining T_e at an oceanic island or seamount of unknown origin it should be possible to estimate whether it formed on young (ridge crest) or old sea floor (off-ridge).

A geophysical observation which can be relatively easily measured on a surface-ship and depends on T_e is the free-air gravity anomaly[7–9,12]. For the theoretical seamount load shown in Fig. 2 there is a significant difference in both amplitude and wavelength between computed gravity anomaly profiles for $T_e = 5$ km, corresponding (Fig. 1) to formation of the load on relatively young sea floor (2–8 Myr), and $T_e = 25$ km, corresponding to formation on relatively old sea floor (>35 Myr). Thus since the overall accuracy of gravity data in the Pacific Ocean is 5–10 mGal (ref. 16), Fig. 2 suggests it should be possible to use observed free-air gravity anomaly profiles to distinguish whether a geological feature originated on a ridge crest or off-ridge.

Data analysis

We have compared observed free-air gravity anomaly profiles obtained on more than 100 cruises of mainly US and USSR research vessels in the Pacific Ocean to calculated profiles based on the elastic plate model. We assumed values of $T_e = 5$ and 25 km since these values clearly represent a ridge crest or off-ridge origin respectively (Fig. 1). The calculated profiles were obtained using linear transfer function techniques[7,9] in which theoretical filters are constructed and convolved with observed bathymetry profiles. Both two- and three-dimensional

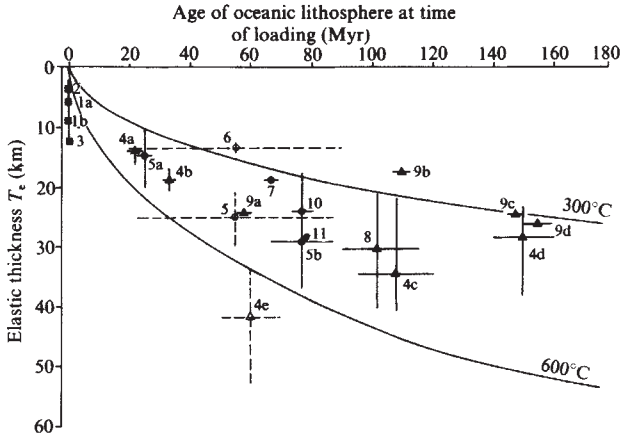

Fig. 1 Plot of elastic thickness of the oceanic lithosphere T_e against age of the lithosphere at the time of loading. 1a, East Pacific rise crest[5]; 1b, Mid-Atlantic Ridge crest[5]; 2, Juan da Fuca ridge crest[6]; 3, Mid-Atlantic Ridge crest[7]; 4, Deep-sea trench outer rise systems[14]; 4a, Nankai trough; 4b, Middle America trench; 4c, Kuril trench; 4d, Mariana trench, 4e, Aleutian trench; 5, Hawaiian–Emperor seamount chain[9]; 5a, Emperor seamounts north of 40° N; 5b, Hawaiian ridge and Emperor seamounts south of 40° N; 6, Pacific Ocean atolls[10] (Cook Islands, Australs, Tuamotu Islands and Henderson); 7, Great Meteor seamount, NE Atlantic[8]; 8, Kuril trench[15]; 9, Deep sea trench-outer rise systems[13]; 9a, Aleutian trench; 9b, Kuril trench; 9c, Bonin trench; 9d, Mariana trench; 10, Hawaiian ridge[11]; 11, Hawaii Island[12]. Each estimate of T_e is related to the flexural rigidity of the plate and is based on an assumed Young's modulus of 1×10^{12} dyn cm^{-2}. The age of the lithosphere at the time of loading was estimated by subtracting the age of each load from the age of the underlying sea floor. For the ridge crest estimates and trench estimates the loading is assumed to be of the present age (0 Myr). For the seamount and oceanic island estimates, the age of loading is obtained from dated samples on the crests or flanks of these features. The solid lines are the 300 °C and 600 °C oceanic isotherms based on a cooling plate model[17].

filters[7] and the effects of non-linearity in the computation of the gravity anomaly have been considered.

Figure 3 shows the comparison between observed and computed gravity anomaly profiles for four selected geological features in the Pacific Ocean. The observed gravity anomaly profiles of the Line Islands ridge and Mid-Pacific mountains can be most satisfactorily explained by the computed profile with $T_e = 5$ km (Fig. 3*a*). The computed profile with $T_e = 25$ km predicts too large an amplitude gravity anomaly over the crest of these features compared with the observed amplitude and wavelengths that are too long over flanking regions. The observed gravity anomaly profiles of Makarov Guyot[3] and Louisville ridge, however, can be most satisfactorily explained by the computed profile with $T_e = 25$ km (Fig. 3*b*). The computed profile with $T_e = 5$ km predicts too small an amplitude over the crest of these features compared with the observed amplitude and wavelengths that are too short over flanking regions.

The comparisons in Fig. 3 can therefore be interpreted as indicating the Line islands ridge and Mid-Pacific mountains formed on a ridge crest (on sea floor of 2–8 Myr age) while Makarov Guyot and Louisville ridge formed off-ridge (on sea floor of >35 Myr age). These conclusions on the origin of these features are, of course, uncertain as they are based on a single gravity anomaly and bathymetry profile and refer only to the origin of the major part of each feature. We have shown[21], however, that uncertainties in the computed profiles, due either to variations in the crustal structure and density of topography assumed or to non-linearity in the computed gravity effects would not significantly alter these conclusions.

Results

The results of the data analysis for each of the cruises in the Pacific Ocean are summarised in Fig. 4: the symbols represent an estimate of the geological setting of an individual bathymetric feature along each ship track. Figure 4*a* summarises those

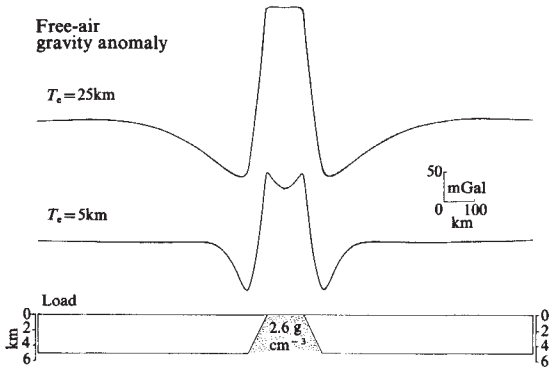

Fig. 2 Computed free-air gravity anomaly profiles based on the continuous elastic plate model and the theoretical seamount load shown. The flexure of the plate has been computed using linear theory[20] and the free-air gravity anomaly has been computed using a two-dimensional line-integral method.

estimates which are interpreted to be of ridge crest origin and Fig. 4*b* those estimates which are of off-ridge origin.

A comparison of Fig. 4*a* with available bathymetry maps of the Pacific Ocean[24,25] show that most of the ridge crest estimates correlate with bathymetric features in the western and central Pacific. These include the Manihiki plateau, Shatsky rise, Hess rise, Necker ridge, Line Islands ridge and Tuamotu Islands and some features in the Magellan seamounts, Mid-Pacific mountains and Emperor seamounts. A number of these features were associated with more than two ridge crest estimates (for example, Shatsky rise (5), Necker ridge (3), Hess rise (4), Line Islands ridge (5) and Tuamotu Islands (10)). Most of the ridge crest estimates (Fig. 4*a*) apparently occur between the 90 and 120 Myr isochrons, based on magnetic anomaly lineations and DSDP sites[22].

The off-ridge estimates (Fig. 4*b*) mainly correlate with bathymetric features in the western Pacific Ocean. These include Society Islands, Samoa, Melanesian border plateau[23], Cross-Line Island trend and Louisville ridge and some features of the Hawaiian ridge and Emperor seamounts, Geisha and Marcus–Wake Guyots[3] and Magellan seamounts. A number of these features were associated with more than two off-ridge estimates (for example, Samoa (3), unnamed seamount in the Magellan seamounts (3), Louisville ridge (3), and Society Islands (3)). The off-ridge estimates show no obvious relationship to the isochrons although the estimates for the Cross-Line Island trend, Hawaiian ridge and Marcus–Wake Guyots correlate with bathymetric features which generally trend WNW–ESE[4], across the local trend of the isochrons.

We recognise that although data from a large number of cruises have been used in this study, the number of estimates in Fig. 4 is small compared with the total number of oceanic islands and seamounts which actually exist in the Pacific Ocean. We believe, however, that although any one estimate in Fig. 4 may be subject to uncertainties, the occurrence of several similar estimates from the same geological feature is evidence that the overall distribution of ridge crest and off-ridge estimates (Fig. 4) is correct. A better test of their reliability, however, is to compare the predicted age of the bathymetric features associated with these estimates to geological ages based on bottom sampling.

The ages of the bathymetric features associated with each estimate (Fig. 4) can be predicted if the age of the underlying sea floor is known (Fig. 1). Table 1 summarises those estimates which are associated with a nearby reliably dated bottom sample. There is a good general agreement between predicted and geological ages for the ridge crest estimates, particularly for Hodgkins, Line Islands, Easter Island and the Tuamotu Islands. The agreement is not as good for the off-ridge estimates because the predicted ages are only maximum estimates.

Table 1 therefore suggests that it should be possible, at least for the ridge crest estimates (Fig. 4*a*), to predict the age of the associated bathymetric features with some confidence. The main uncertainties, however, are in estimating the age of the sea floor, particularly in regions of the magnetic quiet zones. We tabulated the predicted ages for each ridge crest estimate in 30-Myr intervals through geological time. The smallest number of estimates (3) occur for the interval 150–180 Myr BP (Kimmeridgian to Pliensbachian) and the largest number of estimates (26) occur for the interval 90–120 Myr BP (Barremian to Turonian).

The distribution of the off-ridge and ridge crest estimates in the Pacific Ocean basin for the 90–120 Myr BP interval are plotted in Fig. 5. The solid triangles represent ridge crest estimates associated with the Hess rise, Necker ridge, Line Islands ridge, Manihiki plateau and Robbie ridge and the solid circles represent off-ridge estimates associated with the Geisha Guyots, for which there is geological control (Table 1). The bathymetric features associated with the ridge crest estimates extend over a broad region of the Pacific Ocean basin (Fig. 5). We therefore infer that the interval 90–120 Myr BP was a time of significant volcanism on the Pacific plate.

As the solid triangles in Fig. 5 represent ridge crest estimates they may indicate the former position of the accreting Pacific

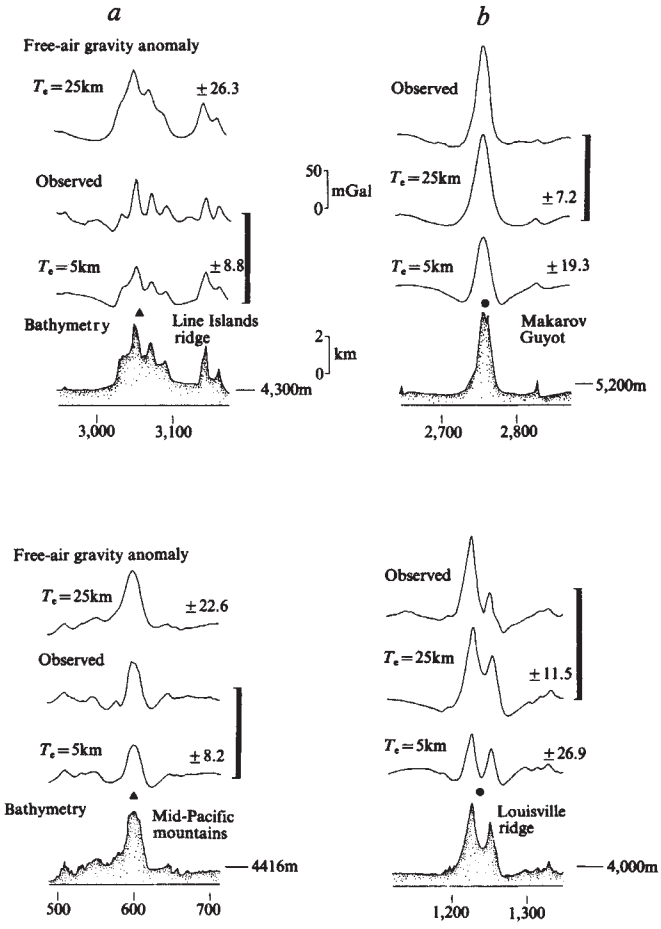

Fig. 3 Comparision of observed free-air gravity anomaly profiles with computed profiles based on the elastic plate model and assumed values of the elastic thickness T_e = 5 km and 25 km. *a*, USNS Eltanin 31 profile of the Line Islands ridge at lat 1.7° N and long 157.0 °W and RV Vema 24 profile of the Mid-Pacific mountains at lat 18.5° N and long 179 5° W. *b*, RV Vema 21 profile of Makarov Guyot at lat 29.6° N and long 153.5° E and USNS Eltanin 40 profile of Louisville ridge at lat 39.3° S and long 167.5° W. The observed profiles of the Line Islands ridge and Mid-Pacific mountains can be best explained by the computed profile of T_e = 5 km and the observed profiles of Makarov Guyot and Louisville ridge can be best explained by the profile for T_e = 25 km. A ridge crest origin (▲) has been assigned to the Line Islands ridge and Mid-Pacific mountains; an off-ridge origin (●) has been assigned to Makarov Guyot and Louisville ridge. The numbers to the right of each computed profile are the r.m.s. differences between observed and calculated gravity anomalies and the number below each bathymetry profile is the distance in nautical miles along a ship track, used to locate each feature.

Table 1 Comparison of predicted ages based on flexure studies with geological ages

Seamount or oceanic island	Ship crossing feature	Position of ship crossing Lat	Long	Method of geological age determination	Position of geological age Lat	Long	Estimated age of underlying sea floor (Myr BP)	Predicted (flexure) age* (Myr BP)	Geological age (Myr BP)	Geological age ref.
Ridge Crest										
Hodgkins (Kodiak–Bowie)	Conrad	53.3	−135.6	K–Ar	53.5	−136.0	17	12±3	14–15	26
Necker ridge	Vema	22.5	−166.7	K–Ar	21.5	−167.9	100	95±3	>61	27
Line Islands	Kana Keoki	3.8	−159.4	DSDP Site 315	4.2	−158.5	102	97±3	91±3	28
Shepard Guyot	Vema	18.5	−179.5	Forams	19.2	−179.5	137	132±3	≥Cen–Tur.	3
Manihiki plateau	Kana Keoki	−12.1	−160.9	DSDP Site 317	−11.0	−162.0	?90	?85±3	≥105	28
Shatsky rise	Conrad	32.1	155.1	DSDP Sites 305, 306	32.0	157.8	136	131±3	≥120	29
Easter Island	Conrad	−27.2	−109.5	K–Ar	Samples from island		4	<2	3	29
Tuamotu	Conrad	−15.6	−147.4	DSDP Site 318	−14.8	−146.8	61	56±3	49–53	30
Wentworth	Kana Keoki	28.8	−177.9	K–Ar	28.8	−177.8	110	105±3	≥71	31
Off-ridge										
Isakov Guyot	Vema	31.6	151.1	Fossil	31.6	151.2	148	<113	≥Lower cretaceous	3
Makarov Guyot	Vema	29.5	153.5	Fossil	29.5	153.3	155	<120	≥Cen–Tur.	3
Z4/3 Guyot†	Vema	27.1	148.7	K–Ar	27.1	148.7	154	<120	≥86–96	32
Lamont Guyot	Argo	21.7	159.4	Fossil	21.5	159.2	170	<135	≥Mid–Eocene	3
Ita Mai Tai Guyot	Dmitri Mendeleyev	12.9	157.0	DSDP sites 200, 202	12.8	156.8	171	<136	≥Early Eocene	33
Somoa (Savaii)	Dmitri Mendeleyev	−13.3	−172.3	Historic eruption	−13.6	−172.4	107	<72	Historic eruption	34
Society	Kana Keoki	−16.1	−151.3	K–Ar	−16.7	−151.0	71	<36	1.9–5.4	35

* Computed assuming a ridge crest estimate corresponds to an age of the lithosphere at the time of loading of 2–8 Myr and an off-ridge estimate corresponds to an age of >35 Myr.

† This seamount has a reliable palaeomagnetic pole[49]. The new constraints on the age suggests this pole (lat. 53.0° N, long. 302°) is probably of early Cretaceous age.

plate boundary. In particular, the Line Islands ridge, Necker ridge and Hess rise probably formed close to the crest of the former Pacific/Farallon plate boundary[36] and the Robbie ridge probably formed close to the crest of the former Pacific/Phoenix plate boundary[36]. Therefore, either volcanism occurred along a major portion of the Pacific plate boundary during 90–120 Myr BP or, beginning about 90–100 Myr BP major ridge jumps occurred along the Pacific plate boundary[4] accompanied by extensive volcanism on the abandoned ridges. Because of the scatter of the ridge crest estimates (Fig. 5) and the fact that only one-limb of the 90–120 Myr BP spreading system is preserved at present, it is not possible to distinguish between these possibilities.

Recent evidence from DSDP site 462[37] and from seismic reflection profiling with a large volume sound source[38] support the earlier suggestion of Winterer[4] that the relatively old crust of the central Pacific basin and the Line Islands area may be obscured by a younger deep-water volcanic event. DSDP site 462[37] (Fig. 5), drilled on oceanic crust of probable late Jurassic age, recovered a volcanic igneous complex of Albian to Aptian age (100–110 Myr BP). Houtz and Ludwig[38] have mapped a seismic reverberant layer, using sonobuoy and single channel vertical incidence data, which reaches thicknesses exceeding 2 km in parts of the central Pacific Ocean basin. Although the reverberant layer may be of calcareous origin[38], the presence of a thick layer (>600 m) in the region of DSDP sites 462 and 169 suggests the layer may be, in part, of volcanic origin and therefore similar in age to the volcanic rocks drilled at the DSDP sites.

These considerations suggest the 90–120 Myr BP ridge crest volcanism which formed the Line Islands ridge, Hess rise and Necker ridge (Fig. 5) may have been accompanied by an extensive deep-water volcanic event in the adjacent ocean basins. The solid line in Fig. 5 outlines the area of the Pacific plate which seems to have been most affected by this event. We have included only evidence from the ridge crest estimates (Fig. 4*a*), the off-ridge estimates for which there is geological control (Table 1) and the contemporaneous deep-water volcanism inferred from DSDP sites and seismic reflection profiling. Thus although other undated oceanic islands and seamounts in the Pacific, not crossed by the cruises, may possibly be of similar age to this event we have not plotted them in Fig. 5.

Discussion

We have documented a major geological event involving an extensive outpouring of ridge crest volcanism on the Pacific plate during the interval 90–120 Myr BP (Barremian to Turonian). This event was probably accompanied by deep-water volcanism. The area of the plate affected by the volcanism is $\sim 10^7$ km^2 (Fig. 5), which is significantly larger than areas of comparable volcanism on the continents (for example, western US since the Miocene[39]).

The origin of the ridge crest volcanism on the Pacific plate during the interval 90–120 Myr BP is not clear at present. The fixed or moving hot-spot hypothesis[40–42] cannot simply explain the volcanism unless a large number of contemporaneous hot spots are proposed along or near the former Pacific/Farallon and Pacific/Phoenix plate boundaries. The lithospheric fracture hypothesis[43] explains the widespread similarity in ages but cannot explain the volcanism unless a stress system is invoked which causes tensional failure of the plate in a direction generally parallel to the trend of the former Pacific/Farallon and Pacific/Phoenix plate boundaries. Thermal contraction of the oceanic plate[44], for example, would cause tensional failure which propagates in the direction of sea floor spreading.

An additional source of stress in the plates, however, are those associated with the driving mechanism of plate tectonics[45]. There is evidence, for example, from magnetic lineation patterns[36] that the 90–120 Myr BP volcanic event on the Pacific plate (Fig. 5) occurred at a time of relatively rapid spreading rate on the Pacific/Farallon ridge crest. This spreading rate increase, if it occurred[46], may have been accompanied by either the initiation of subduction or an increase in the convergence rate on another Pacific plate boundary. If this increase in convergence rate was accompanied by an increase in the driving force on the subducting plate[47], additional stresses may have been transmitted to the horizontal part of the plate. These stresses may have been sufficient to cause the Pacific plate to fracture at its weakest point and allow magma to flow from the underlying asthenosphere to the area around the ridge crest.

We have also documented the distribution of off-ridge volcanism on the Pacific plate (Fig. 4*b*). As some of the estimates of off-ridge volcanism are from the oldest part of the Pacific plate (Fig. 4*b*) this volcanism is therefore of late Jurassic or younger age. The main problem, however, is that with the exception of

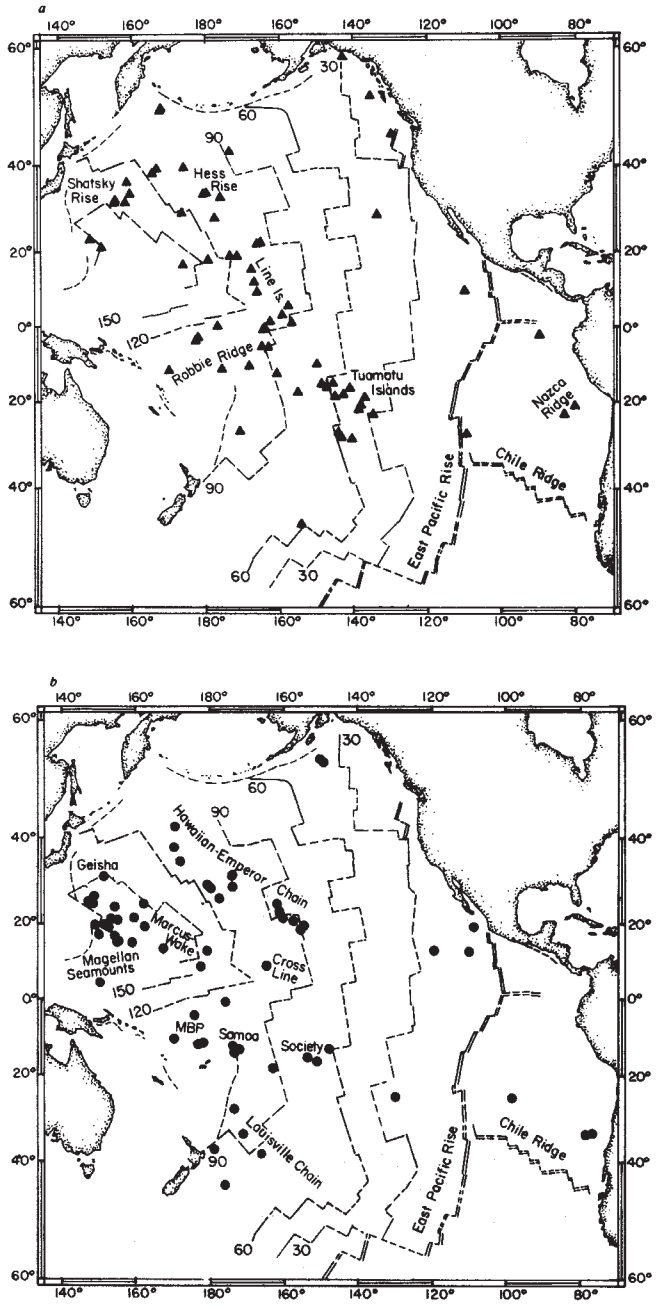

Fig. 4 Plot of estimates of ridge crest (*a*) and off-ridge volcanism (*b*) on the Pacific plate. The solid lines indicate isochrons based on observed magnetic lineations and DSDP sites and the dashed lines indicate interpolated isochrons based on tectonic reconstructions for the Pacific plate[22]. MBP, Melanesian border plateau[23].

the Hawaiian–Emperor seamounts and some features in the Geisha Guyots, where there is adequate geological control, the age of the off-ridge volcanism is generally unknown (for example, Table 1).

There is evidence, however, that at least part of the off-ridge volcanism in Fig. 4*b* may be of younger age than 90–120 Myr BP. The Line Islands ridge between latitudes 5°N and 15°N are intersected by the WNW–ESE Cross-Line Island trend which, based on bathymetry[4] and the estimated age of the off-ridge estimate at latitude 12°N longitude 165°W (Fig. 4*b*), are younger than the Line Islands ridge. The Melanesian border plateau, Samoa and Society Islands, which seem to form part of a broad WNW–ESE trend in off-ridge volcanism in the central Pacific (Fig. 4*b*), are probably younger than middle Cretaceous (see Table 1). The age of the off-ridge volcanism of the Magellan seamounts and Marcus–Wake Guyots is not known, however, although they are associated with similar WNW–ESE trends in bathymetry as the Cross-Line Island trend[4,24].

The presence of WNW–ESE trends in the bathymetry of features associated with off-ridge volcanism (Marcus–Wake Guyots, Magellan seamounts, Cross-Line Island trend) is of particular interest as they cross isochrons and are generally parallel to the direction of present day absolute Pacific plate motions. One possibility therefore is that the off-ridge volcanism

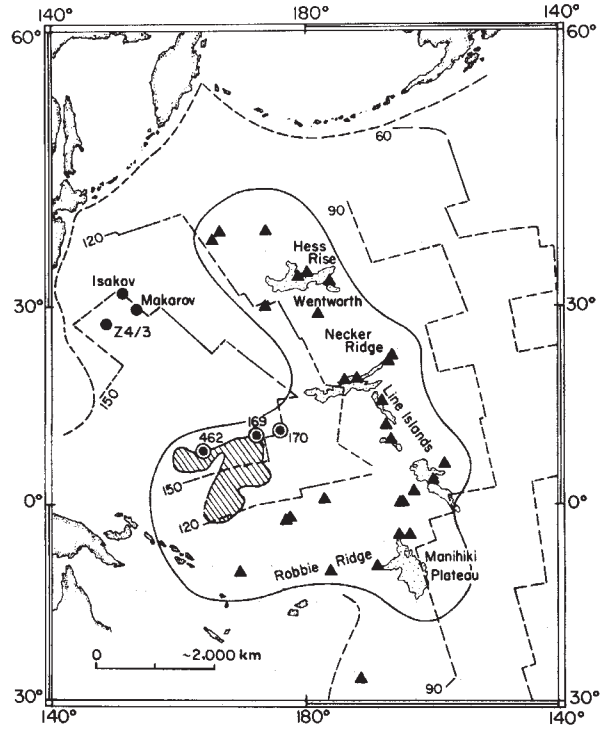

Fig. 5 Map summarising the inferred distribution of volcanism on the Pacific plate during the interval 90–120 Myr BP (Barremian to Turonian). ▲, Bathymetric features formed at a ridge crest; ●, features formed off-ridge. The ridge crest features probably originated on or near the Pacific/Farallon and Pacific/Phoenix ridge crests[36] and the off-ridge features originated in the interior of the Pacific plate away from the accreting plate boundaries. ⊙, The deep water DSDP sites which were drilled on oceanic crust of probable late Jurassic age and sampled basaltic igneous rocks of Albian to Aptian age (100–110 Myr BP). The shaded area is the >600-m isopach of the seismic reverberant layer[38] in the region of DSDP sites 462 and 169 and the stippled area indicates the extent of shallow (<4,000 m)[24] sea floor in the region of the Manihiki plateau, Line Islands ridge, Necker ridge, Hess rise and Mid-Pacific mountains.

is a surface expression of small-scale convection[48] in the underlying mantle. The ages of these features are not well enough known, however, and more studies need to be carried out before this possibility can be examined.

We thank R. D. Jarrard for special assistance. This work was supported by NSF grant OCE 77-07941 and Office of Naval Research contract N00014-75-C-210 Scope C.

Received 3 August; accepted 28 November 1979.

1. Menard, H. W. & Ladd, H. S. in *The Sea* **3**, 365 (1963).
2. Menard, H. W. *Marine Geology of the Pacific* (McGraw-Hill, New York, 1964).
3. Heezen, B. C. *et al. Init. Rep. DSDP* **20**, 652 (1973).
4. Winterer, E. L. *Am. geophys. Un. Monogr.* No. 19, 269 (1976).
5. Cochran, J. R. *J. geophys. Res.* **84**, 4713 (1979).
6. McNutt, M. *J. geophys. Res.* (in the press).
7. McKenzie, D. P. & Bowin, C. *J. geophys. Res.* **81**, 1903 (1976).
8. Watts, A. B., Cochran, J. R. & Selzer, G. *J. geophys. Res.* **80**, 1391 (1975).
9. Watts, A. B. *J. geophys. Res.* **83**, 5989 (1978).
10. McNutt, M. & Menard, H. W. *J. geophys. Res.* **83**, 1206 (1978).

11. Suyenaga, W. thesis, Univ. Hawaii (1977).
12. Walcott, R. I. *Tectonophysics* **9,** 435 (1970).
13. Caldwell, J. G., Haxby, W. F., Karig, D. E. & Turcotte, D. L. *Earth planet. Sci. Lett.* **31,** 239 (1976).
14. Caldwell, J. G. thesis, Cornell Univ. (1979).
15. McAdoo, D. C., Caldwell, J. G. & Turcotte, D. L. *Geophys. J. R. astr. Soc.* **54,** 11 (1978).
16. Watts, A. B., Talwani, M. & Cochran, J. R. *Am. geophys. Un.* Monogr. No. 19, 17 (1976).
17. Parsons, B. & Sclater, J. G. *J. geophys. Res.* **82,** 803 (1977).
18. Anderson, D. L. & Minster, J. B. *Phys. Earth Planet. Int. Proc. Jean Coulomb Symp.* (in the press).
19. Goetze, C. & Evans, B. R. *Geophys. J. R. astr. Soc.* (in the press).
20. Hetènyi, M. *Beams on Elastic Foundation* (The University of Michigan Press, Ann Arbor, 1964).
21. Watts, A. B., Bodine, J. H. & Ribe, N. (in preparation).
22. Pitman, W. C., Larson, R. L. & Golovchenko, X. (in preparation).
23. Fairbridge, R. W. *Dt Hydrogr. Z.* **15,** 1 (1962).
24. Chase, T. E., Menard, H. W. & Mammerickx, J. *IMR Techn. Rep. Ser.* TR-17 (1970).
25. Mammerickx, J., Smith, S. M., Taylor, I. L. & Chase, T. E. *IMR Tech. Rep. Ser.* TR-56 (1975).
26. Turner, D. L., Forbes, R. B. & Naeser, C. W. *Science* **182,** 589 (1973).
27. Natland, J. H. *Init. Rep. DSDP* **33,** 749 (1976).
28. Lanphere, M. A. & Dalrymple, G. B. *Init. Rep. DSDP* **33,** 649 (1976).
29. Scientific staff *Init. Rep. DSDP* **32, 75** and **159** (1975).
30. Scientific Party *Geotimes* **19,** 17 (1974).
31. Clague, D. A. & Dalrymple, G. B. *Geophys. Res. Lett.* **2,** 305 (1975).
32. Ozima, M., Kaneoka, I. & Aramaki, S. *Earth planet. Sci. Lett.* **8,** 237 (1970).
33. Scientific Party *Init. Rep. DSDP* **20,** 87 (1973).
34. Richard, J. J. *Int. Volcanol. Ass.* Naples (1962).
35. Krummenacher, D. & Noetzlin, J. *Bull. geol. Soc. Fr.* **8,** 173 (1966).
36. Larson, R. L. & Pitman, W. C. *Bull. geol. Soc. Am.* **83,** 3645 (1972).
37. Scientific Party *Geotimes* **23,** 21 (1978).
38. Houtz, R. & Ludwig, W. *J. geophys. Res.* **84,** 3497 (1979).
39. King, P. B. & Beikman, H. M. *Geological Map of the US* (US Geological Survey, 1974).
40. Morgan, W. J. *Bull. Am. Ass. Petrol. Geol.* **56,** 203 (1972).
41. Burke, K., Kidd, W. S. F., & Wilson, J. T. *Nature* **245,** 133 (1973).
42. Minster, J. B., Jordan, T. H., Molnar, P. & Haines, E. *Geophys. J. R. astr. Soc.* **36,** 541 (1974).
43. Turcotte, D. L. & Oxburgh, E. R. *Phil. Trans. R. Soc.* **A288,** 561 (1978).
44. Turcotte, D. L. *J. geophys. Res.* **79,** 2573 (1974).
45. Forsyth, D. & Uyeda, S. *Geophys. J. R. astr. Soc.* **43,** 163 (1975).
46. Berggren, W. A., McKenzie, D. P., Sclater, J. G. & Van Hinte, J. E. *Bull. geol. Soc. Am.* **86,** 267 (1975).
47. Richter, F. M. & McKenzie, D. P. *J. Geophys.* **44,** 441 (1978).
48. Richter, F. M. *J. geophys. Res.* **78,** 8735 (1973).
49. Harrison, C. G. A., Jarrard, R. D., Vacquier, V. & Larson, R. L. *Geophys. J. R. astr. Soc.* **42,** 859 (1975).

In vitro and *in vivo* products of *E. coli* lactose permease gene are identical

Ruth Ehring & Konrad Beyreuther

Institut für Genetik der Universität zu Köln, Weyertal 121, D5000 Köln 41, FRG

J. Keith Wright & Peter Overath

Max-Planck-Institut für Biologie, Correnssstr. 38, D7400 Tübingen, FRG

The lacY *gene product synthesised* in vitro *is identical to lactose permease isolated from cytoplasmic membranes as determined by apparent molecular weight and N-terminal amino acid sequence. The amino acid composition of the* in vivo *product agrees well with that predicted from the DNA sequence. The data assign the translational start on the DNA sequence and demonstrate that this protein is processed only by deformylation but not by proteolytic cleavage at the N-terminus.*

IN both bacterial and eukaryotic cells, most secreted proteins are initially synthesised as precursors with hydrophobic amino-terminal extensions which are removed by proteolytic cleavage during or after translocation of the protein through the membrane[1,2]. Such precursors have been demonstrated for some integral membrane proteins, such as the coat protein of the bacteriophage M13 (refs 3, 4), whereas in other cases the primary translation product formed *in vitro* seems to be identical to the membrane-associated *in vivo* product[5,6]. We describe here the *in vitro* synthesis of lactose permease (lactose carrier, product of the *Y* gene of the *lac* operon) of *Escherichia coli*[7] and show that the *in vitro* product is identical to permease isolated from the cytoplasmic membrane of this organism. As a model for the biosynthesis of a hydrophobic protein, lactose permease seems particularly attractive because this protein must attain a highly organised tertiary structure in the membrane in order to function as a lactose/proton-symporter[8].

Cell-free protein synthesis directed by hybrid plasmid pGM21

pGM21 is a hybrid plasmid between the vector pACYC 184 (ref. 9) and a previously described *lac Y* gene-containing fragment[10,11] integrated into the single site for the restriction enzyme *Eco*RI located in the gene conferring resistance to chloramphenicol. The fragment comprises about 2,300 base pairs and carries an intact *lac* promoter and operator region, an intact *Y* gene, but only minor parts of the *A* (thiogalactoside transacetylase), *Z* (β-galactosidase) and *I* (repressor) genes [genotype $lac\Delta(I)P^{+}O^{+}\Delta(Z)Y^{+}\Delta(A)$]. The restriction maps of this fragment and the *lac Y* gene-containing fragment sequenced in the preceding paper[12] are identical in the region of the *Y* gene. *In vivo*, pGM21-directed synthesis of lactose permease is inducible. The protein comprises up to 15% of the cytoplasmic membrane protein and is functionally intact as judged by transport and substrate binding experiments[10,13,14].

When added to a coupled transcription–translation system according to Zubay *et al.*[15], plasmid pGM21 efficiently promotes cell-free protein synthesis. In an incubation mixture containing ^{14}C-phenylalanine as the only radioactive amino acid, 11% of the label is found in a high molecular weight (MW) form, whereas in the absence of pGM21 only 0.1% of the input radioactivity becomes acid precipitable. An aliquot of the total incubation mixture was analysed on a polyacrylamide gel (Fig. 1*a*). It is clear that pGM21 directs the synthesis of one major product (slice nos 36–42, 33% of radioactivity) of apparent MW 30,000 ± 1,000. This radioactive peak corresponds in both mobility and width to purified lactose permease (prominently stained band in gel at the top of Fig. 1) or permease labelled with ^{3}H-*N*-ethylmaleimide in intact cytoplasmic membranes (Fig. 1*b*). Thus, the main product of the *in vitro* synthesis is identical to lactose permease within the resolution of the method.

As pGM21 contains an intact promoter–operator region, *in vitro* expression of the *Y* gene should be stimulated by cyclic AMP and reduced by *lac* repressor. Furthermore, repression should be relieved by addition of the inducer isopropyl β-D-thiogalactopyranoside (IPTG). Analysis of *in vitro* protein synthesis reaction mixtures on acrylamide gels demonstrates that the major product (apparent MW 30,000) is indeed subject to regulation by cyclic AMP and repressor (compare lanes 6–9 of Fig. 2). In terms of total incorporation of radioactive amino acids into protein (see Fig. 2 legend), cyclic AMP stimulates about twofold, repressor suppresses this synthesis by 60%, and addition of IPTG relieves the inhibition almost completely. These effects of cyclic AMP and repressor are small compared with control studies on *in vitro* synthesis of β-galactosidase directed by DNA from *lac* transducing phage λ in the same conditions. As quantitated by catalytic activity, the synthesis of this enzyme

0028-0836/80/060537—04$01.00